Solar Phys (2007) 241: 397–409
DOI 10.1007/s11207-007-0348-x

Coronal Periodmaps

Automated Detection of Wave and Oscillatory Phenomena in Coronal Imaging Data

V.M. Nakariakov · D.B. King

Received: 2 November 2006 / Accepted: 1 March 2007 /
Published online: 26 April 2007

Abstract The search for signatures of wave and oscillatory processes in the solar corona in the data obtained with imaging instruments can be automated by using the periodmap method. The method reduces a three-dimensional data cube to a two-dimensional map of the analysed field of view. The map reveals the presence and distribution of the most pronounced frequencies in the power spectrum of the time signal recorded at spatial pixels. We demonstrate the applicability of this method as a pre-analysis tool with the use of TRACE EUV coronal data, which contain examples of transverse and longitudinal oscillations of coronal loops. The main advantage of using periodmaps over other possible (more sophisticated) pre-analysis tools, such as wavelet analysis, is their robustness and efficiency (both in speed and computational power). The method can be implemented in the Hinode/XRT and SDO/AIA data pre-analysis.

Keywords Coronal oscillations · Coronal waves · MHD waves · EUV

1. Introduction

The recent avalanche of observational discoveries and identifications of various magnetohydrodynamic (MHD) modes in solar coronal structures has made the study of waves and oscillations a mainstream activity of coronal physics (see Nakariakov and Verwichte, 2005 for a review). A significant portion of these discoveries has been made with imaging telescopes (SOHO/EIT, TRACE and the Nobeyama Radioheliograph (NoRH)) operating in the EUV and microwave bands. So far, the search for events, interesting for a more detailed analysis (the *pre-analysis* of the data), has been carried out "by eye" — the researcher had to scan "manually" full-resolution data cubes, looking for oscillatory patterns. Obviously, this approach cannot be considered either as efficient or robust, especially if one takes into account that some coronal oscillatory events, such as propagating and standing longitudinal modes, are not associated with flaring energy releases. Solar coronal wave studies would

V.M. Nakariakov (✉) · D.B. King
Physics Department, University of Warwick, Coventry CV4 7AL, UK
e-mail: V.Nakariakov@warwick.ac.uk

certainly benefit from the development and implementation of *pre-analysis* tools for the automated detection of wave and oscillatory phenomena in imaging data cubes. The expected outcome of an automated detection method is a reduction of the analysed data cube to a 1D or 2D signal, showing spatial or temporal location of harmonic patterns. The tools for the pre-analysis should not be confused with the data analysis tools. The main qualities of a pre-analysis tool are its robustness (the majority of the phenomena of interest should be findable with the method), the calculation speed (*e.g.* the time taken to pre-analyse the data set should be shorter than the duration of the observation) and its clear and simple outcome. The upcoming high-cadence large field-of-view data from imaging instruments Hinode/XRT and SDO/AIA makes this task even more timely.

Coronal variability has been intensively studied in the context of flare statistics, and there have been several methods designed for the automated detection of microflares. In particular, there have been several studies of the automated reduction of coronal imaging data cubes to lower-dimensional signals. For example, Aschwanden *et al.* (2000) developed a technique for the automated detection of spatio-temporal variability of TRACE EUV data cubes, applicable to the quiet regions of the corona. The aim of the technique was the automated search for coronal energy release events. The time variability was characterised by measuring the maximum flux change, defined by the difference of the maximum and minimum in a time series coming from a macropixel consisting of 4×4 pixels. The macropixels with the maximum flux change exceeding a certain prescribed threshold were put on a map. Then, spatially neighbouring macropixels that demonstrated coherent time evolution were used to discriminate between individual energy-release events.

A technique for the automated detection of EIT waves (also called coronal Moreton waves) and propagating EUV dimmings was developed by Podladchikova and Berghmans (2005). Their method is based upon the accepted observational fact that this phenomenon has a clear polar symmetry. The method outcome is a structure map of the pre-analysed data cube, which reveals the presence of the phenomenon in the data. This technique is designed for the study of propagating large-amplitude perturbations of polar symmetry, and thus it cannot be applied to the pre-analysis of other wave and oscillatory phenomena.

Recently, Grechnev (2003) proposed a technique for the creation of a 2D variance map, representing the overall dynamics of the analysed event, from microwave correlation data cubes obtained with NoRH. This approach helps to reveal faint variable microwave emission sources. However, coronal EUV data cubes are known to contain many highly variable features and structures, and it is not clear whether the variance mapping technique can be successfully applied to these data, especially for the detection of wave and oscillatory processes.

Coronal EUV data sets are often not evenly sampled in time, and the exposure and cadence times can vary quite significantly. Also, one of the main problems with the automated detection of coronal wave and oscillatory processes is that even clearly harmonic wave-like motions observed in the solar corona last only a few periods. De Moortel and McAteer (2004) developed a technique based upon the wavelet transform for automating the detection of longitudinal propagating waves. This approach was found to be successful in picking up both short-lived and sustained periodicities. The detection method was based upon the technique developed by Ireland *et al.* (1999) and McAteer *et al.* (2003). For each pixel, periodogram (Fourier power spectrum) peaks over a prescribed confidence level were searched for. Then, the duration of each periodicity was determined. If the duration was found to be longer than $\sqrt{2}P$, where P is the detected period, this periodicity was considered as an "oscillation". Using a wavelet analysis enables the detection of both long-lived oscillatory events (*e.g.* propagating longitudinal waves in magnetic fans) and transient phenomena (*e.g.*

transverse oscillations of loops). However, this technique has two shortcomings: the calculation time and the visualisation of the results, as the technique's output still has the time coordinate. Pre-analysis of large full-sun EUV imaging data cubes, such as planned with SDO/AIA (see, *e.g.* Title *et al.*, 2006), requires a simpler and less time consuming technique for the oscillation detection.

In this paper, we test the applicability of the variance mapping techniques to coronal EUV imaging data cubes. Then, we evaluate a method for the detection of wave and oscillatory processes in coronal EUV imaging data cubes, based upon the transformation of analysed three-dimensional data cubes to two-dimensional periodmaps. We present a *proof of principle* by testing the periodmap method on an artificial signal and on well-known TRACE 171 and 195 Å data cubes, which contained examples of transverse oscillations and propagating longitudinal waves.

2. Analysed Signals

In this study we test the proposed method by analysing two kinds of data: simulated imaging data cubes with built-in periodicity and noise and EUV coronal data cubes obtained with TRACE.

2.1. Simulated Data Cubes

We constructed an artificial data cube as follows: The simulated image has a rectangular shape of size L_x by L_z. The images are taken with cadence t_{cad}. Each pixel is assigned a background intensity $\mathcal{I}_0^{\mathrm{sim}}$. In the image, there is a straight vertical (the z-direction) stripe, simulating a loop, of Gaussian shape with the variable width w_{vis}. The loop brightness is enhanced near its apex, having a Gaussian shape that is controlled by a parameter L_{vis}. The loop oscillation is set up in the form of a global kink mode with amplitude A^{sim}, period P^{sim} and decay time $t_{\mathrm{dec}}^{\mathrm{sim}}$. Thus, the loop displacement is modelled by the signal

$$s(z,t) = A^{\mathrm{sim}} \cos(\pi z/L_z) \sin\bigl(\pi t/P^{\mathrm{sim}}\bigr) \exp\bigl(-t/t_{\mathrm{dec}}^{\mathrm{sim}}\bigr). \tag{1}$$

The combined (signal plus background) brightness is given by the equation

$$\mathcal{I}^{\mathrm{sim}} = \mathcal{I}_0^{\mathrm{sim}} + \exp\left(-\frac{(x-s)^2}{w_{\mathrm{vis}}^2}\right) \exp\left(-\frac{z^2}{L_{\mathrm{vis}}^2}\right) + A_{\mathrm{n}} f_{\mathrm{n}}(x,z,t), \tag{2}$$

where the last term represents noise given by a function f_{n} with amplitude A_{n}. The function f_{n} can be one of the random noise generators built into the Interactive Data Language (IDL) package (*e.g.* the function *randomn*).

Thus, this model allows us to control the parameters of the loop (the width w_{vis}, the relative brightness i^{sim} and the longitudinal decrease of the brightness L_{vis}) and of its oscillations (the displacement amplitude A^{sim}, period P^{sim} and decay time $t_{\mathrm{dec}}^{\mathrm{sim}}$), as well as the noise-level amplitude A_{n}.

2.2. TRACE Data Cubes: Transverse Oscillations

As natural data examples, we use 171 and 195 Å TRACE data cubes recorded from 12:00 UT to 14:00 UT on 14 July 1998 (the Bastille Day event in 1998), which contain

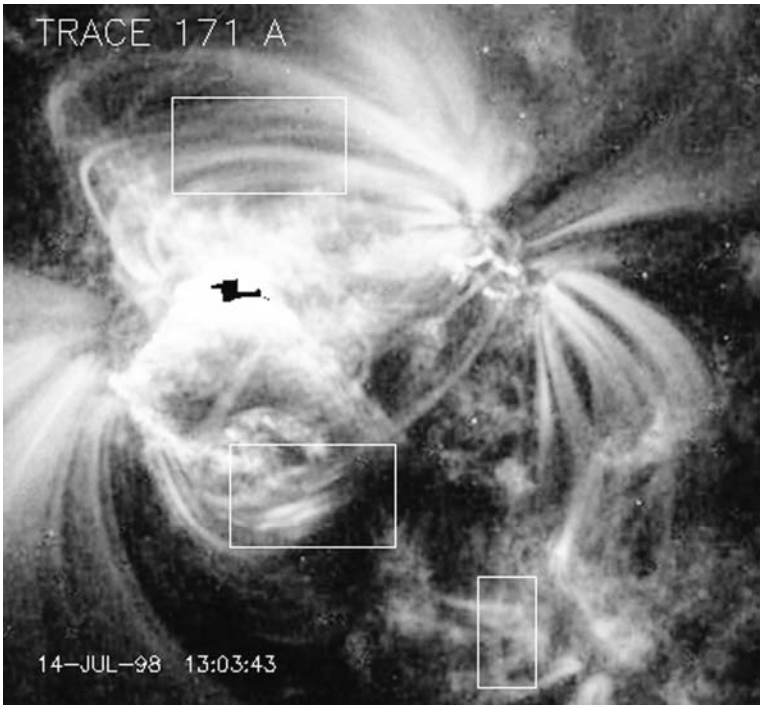

Figure 1 An image of the AR8270 in 171 Å. EUV movies of this active region recorded with TRACE from 12:00 UT to 14:00 UT on 14 July 1998 are used as examples. White boxes show the parts of the active region where clear transverse oscillations are seen.

well-pronounced transverse oscillations of coronal loops situated in the active region 8270 (see Aschwanden *et al.*, 1999; and Nakariakov *et al.*, 1999 for the detailed analysis of this event and the oscillations). The characteristic periods of the oscillations were 4 to 6 min, the displacement amplitudes were, according to Aschwanden *et al.* (1999), 4.1 ± 1.3 Mm and the decay times were 10 – 15 min. The mean cadence time was about 75 s for both 171 and 195 Å images, with standard deviations of about 2.8 and 2.0 s, respectively, with the exception of one missing frame. The oscillations are observed after an M4.6 flare, which started at about 12:55 UT.

The data were preprocessed with the use of the *trace_prep* subroutine of SSW IDL, which performed despiking, destreaking and deripplingand subtracted the dark pedestal and current and normalised for exposure (*/wave2point, /unspike, /destreak, /deripple, /normalize, /float*).

Figure 1 shows the analysed field of view (FOV) as seen in the 171 Å bandpass. The white boxes show those regions where it is possible to detect visually the quasi-periodic transverse displacements (transverse oscillations) of the coronal loops.

2.3. TRACE Data Cubes: Propagating Longitudinal Waves

Another wave phenomenon often observed in the corona is the propagation of longitudinal waves. A typical event of this kind was analysed by King *et al.* (2003). The longitudinal waves were observed by TRACE in both 171 and 195 Å on 2 July 1998 in the active region

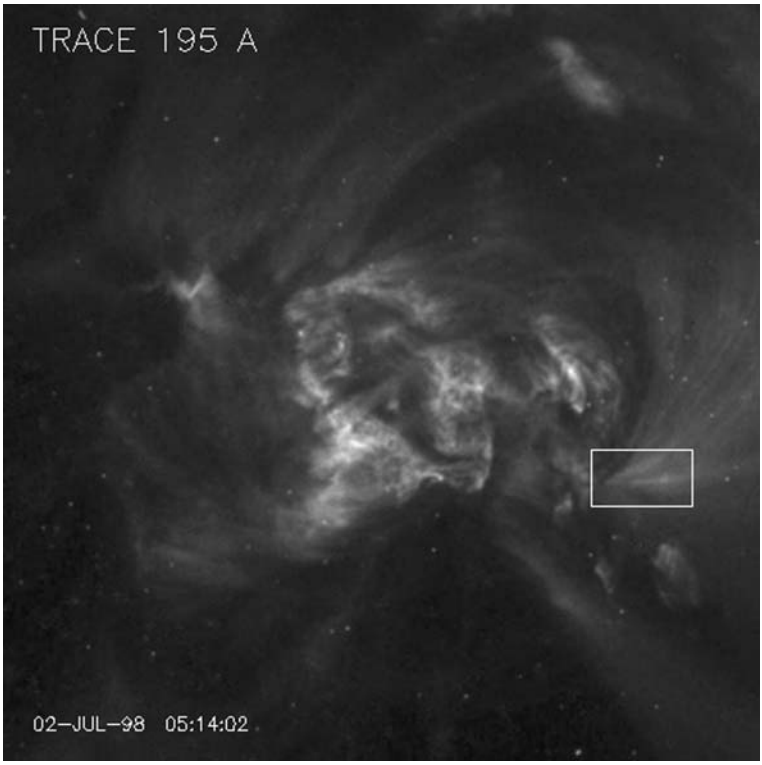

Figure 2 An image of the AR 8253 in 195 Å. EUV movies of this active region recorded with TRACE from 06:00 UT to 07:00 UT on 2 July 1998 show propagating longitudinal waves in the magnetic fan region (highlighted by the white box).

AR 8253 for about an hour beginning at 6:00 UT. In both bandpasses the cadence time was 31 s and the delay time between images taken in 195 and 171 Å was 11 s. The event was not associated with any flare. The data cube was pre-processed identically to the data set discussed in the previous subsection.

3. Variance Maps

The method of variance maps proposed and developed by Grechnev (2003) for NoRH data cubes can be applied to TRACE EUV data cubes as well. The idea of the method is the following. For each pixel (i, j), the variance of the time-dependent intensity is calculated,

$$\sigma_{ij}^2 = \frac{1}{N_t}\sum_{t=0}^{N_t-1}\mathcal{I}_{i,j,n}^2 - \frac{1}{N_t^2}\left(\sum_{t=0}^{N_t-1}\mathcal{I}_{i,j,n}^2\right)^2, \tag{3}$$

where the index n is the index of the time frame and N_t is the number of frames in the data cube analysed. Strictly speaking, this expression is different from the standard definition of the variance, as the cross-terms are missing. According to Grechnev (2003), the cross-terms are skipped to avoid scanning the data cube twice and hence to decrease the calculation time.

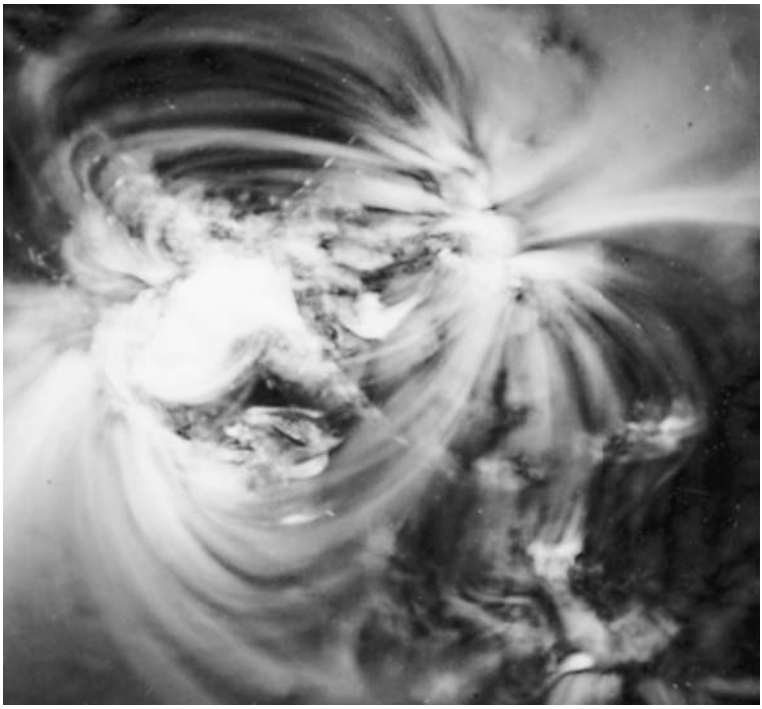

Figure 3 The variance map of the data cube recorded by TRACE in 171 Å from 12:00 UT to 14:00 UT on 14 July 1998.

Figure 3 shows the variance map of the data cube described in Section 2.2. Apparently, it is impossible to distinguish between the oscillating and nonoscillating regions on the map, as the entire field of view is highly variable. This is a common feature of EUV coronal data sets. Thus, the variance mapping technique does not seem to be useful for the pre-analysis of EUV data cubes, in contrast with microwave imaging data, which usually contain just a few sources of time-varying microwave emission.

4. Periodmaps

We propose an alternative method for pre-analysis of EUV imaging coronal data cubes, based upon the reduction of the original data cube to a 2D map of the analysed FOV. On the map, the pixel colour corresponds to the period of the highest peak in the power spectrum of the time signal coming from this pixel, provided the peak amplitude exceeds some certain prescribed threshold. Otherwise, the pixel is shown in black. This technique has already been applied in solar physics as a data *analysis* tool. In particular, Terradas *et al.* (2002) used this technique for processing 2D Dopplergrams in the study of prominence oscillations. However, to the best of our knowledge, this approach has not been either proposed or tested as a pre-analytical tool for the automated detection of oscillatory patterns in the solar corona.

Figure 4 shows a typical spectrum of a pixel that belongs to an area covered by a transverse oscillation of a coronal loop. One of the possible criteria of periodicity detection is to accept the maximum value of the spectral function as the signal if the value is N_{thres} times

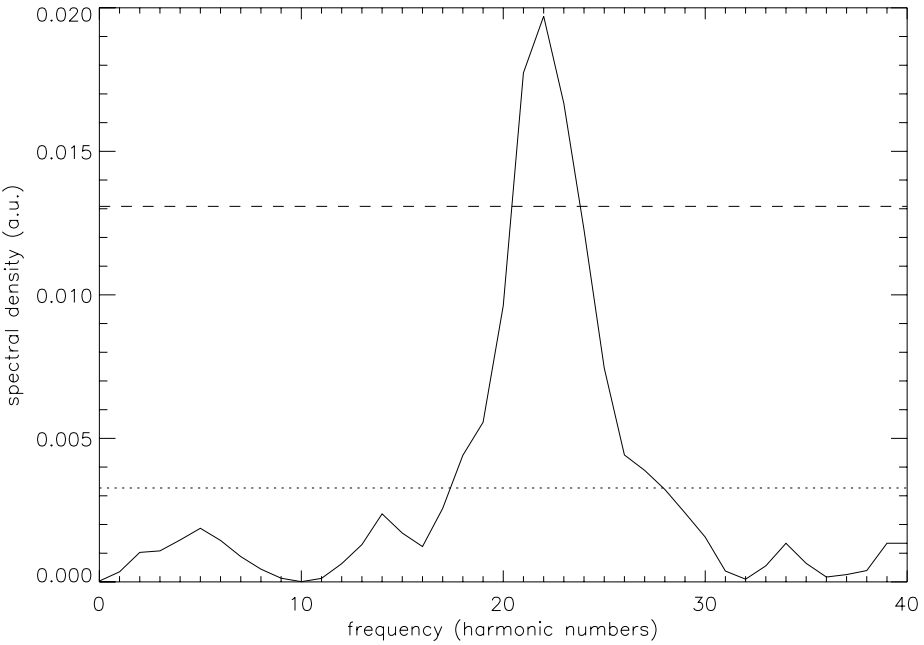

Figure 4 A power spectrum of an EUV signal from a TRACE image pixel. The dotted line corresponds to the mean value of the function, and the dashed line to the mean value multiplied by a factor of 4, which is a prescribed periodicity detection criterion.

greater than the mean value of the spectral function. In practice, for TRACE signals, the value of N_{thres} may be about 3 or 4.

A more rigorous approach requires the calculation of the detection probability levels for the analysed spectra (*e.g.* Monte Carlo simulations implementing the method of Fisher randomisations). Detailed discussion of this operation is given in O'Shea *et al.* (2001). In practice, the application of this method requires the calculation of power spectra of at least 150 permutations of original signals, which increases the calculation time by 150 times. Thus, unfortunately, the application of the randomisation technique leads to an enormous increase in the calculation time and cannot be implemented in a pre-analysis tool.

We propose an alternative method for the assessment of the false alarm probability in imaging data. As modern EUV imagers allow us to resolve oscillating coronal structures spatially, the image of the oscillating structure consists of several pixels. The proposed method is based upon the assumption that if there is no harmonic signal in the analysed data, the probability that the same spectral peak, *i.e.* at the same frequency, appears at several neighbouring pixels would be low. If the structure, *e.g.* a loop, oscillates at a certain MHD mode, the oscillatory signal would be present in the majority of the pixels resolving the structure, even when the noise level is high. The "false alarm" probability, defined as the probability that M neighbouring pixels accidentally have a spectral maximum at the same frequency, is $(2/N_t)^{M-1}$, where N_t is the number of time frames in the data cube. We determine the amplitude of the maximum of the spectrum by measuring it in the units of mean values of the spectrum. If the spectral amplitude is below some prescribed threshold, we consider this as an absence of periodicity. In the case when several neighbouring pixels have acceptable spectral maxima at the same (or, possibly, similar) frequency, there is a chance that the pe-

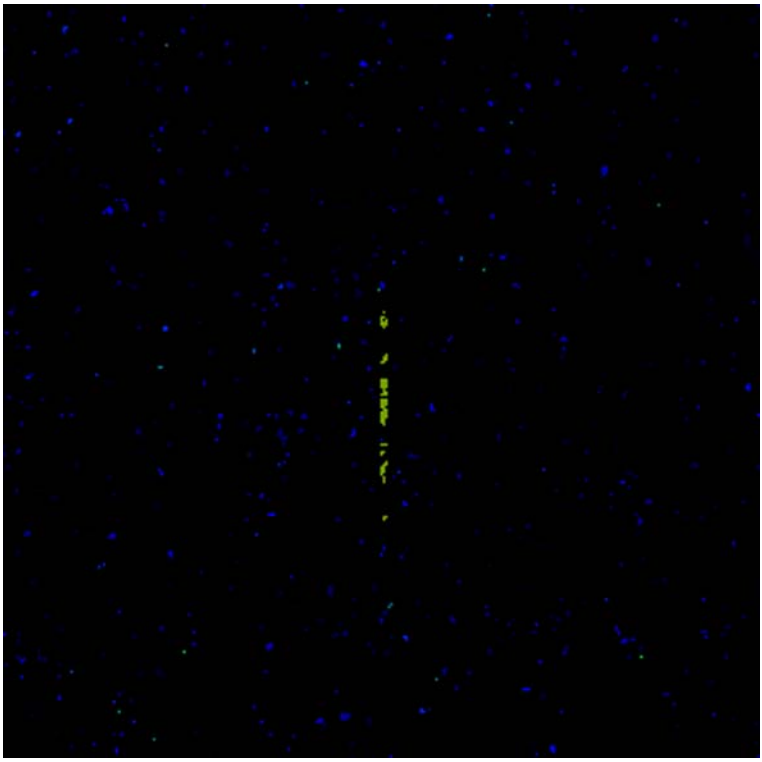

Figure 5 Periodmap of a simulated data cube with an oscillating loop. The loop width is 2 Mm, the oscillation period is 300 s, the displacement amplitude is 5 Mm, the decay time is 1 800 s, and the noise amplitude is three times higher than the loop brightness. The data cube has 100 frames with the cadence time of 31 s.

riodicity still happens accidentally, because of the time correlation of the signals at those pixels. However, even if a certain group of pixels is present on the periodmap because of a false alarm, the high correlation of the signals at those pixels is worthy of closer attention.

Thus, for each pixel of the analysed data cube, we calculate the spectrum of its time signal (made from the original signal by subtracting a best-fitting parabolic function to get rid of the slow varying trend), determine its maximum and the mean value and, if the maximum value is greater than the mean value by some prescribed factor (*e.g.*, good results are obtained when it is 3 or 4), we assign this pixel a colour corresponding to the frequency of the maximum, according to a chosen colour table. Otherwise, the pixel is assigned a zero frequency, or, in other words, is blank. As an alternative, we can calculate the spectrum of the running difference of the signal. The running difference corresponds to taking the time derivative of the signal, which detrends any linear background trend. Also, we perform some filtering of the analysed signal. If the analysed signal has the highest spectral peak outside the range of the frequencies $f_{\min} < f < f_{\max}$ the pixel is assigned a zero frequency. Typically, we subtract the three highest and three lowest harmonics in the spectrum.

Figure 5 shows the periodmap of the simulated signal discussed in Section 2.1. The colour of the pixels with spectral maxima greater than a prescribed threshold (equal to 4) is assigned according to the IDL colour table "PRISM" (number 6). The red colour corresponds to longer periodicities and the violet colour corresponds to shorter periodicities,

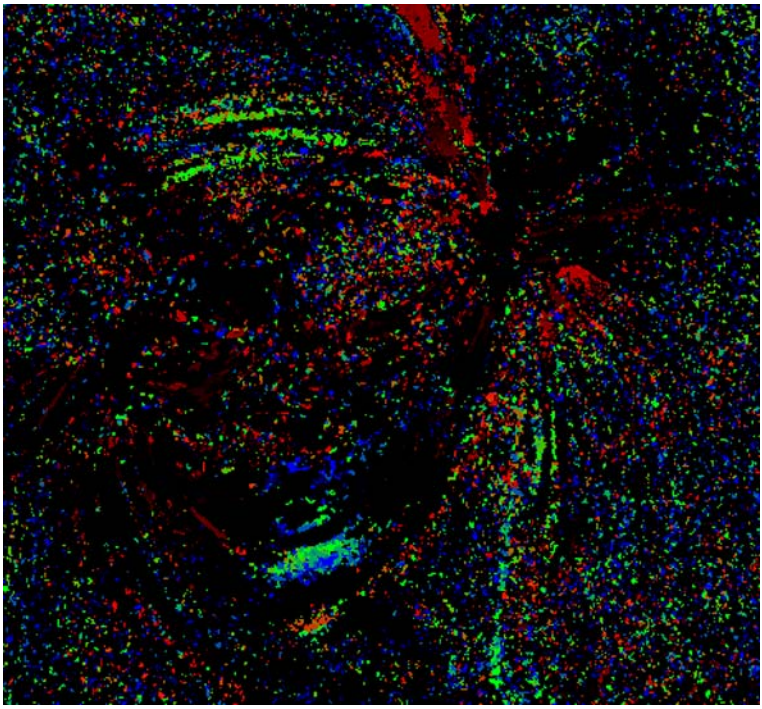

Figure 6 Periodmap of the data cube recorded by TRACE in the 171 Å bandpass for the event on 14 July 1998.

which are close to the Nyquist frequency. The prescribed period of the loop oscillations, 300 s, corresponds to the green colour. The oscillating loop is clearly resolved *by eye* on the periodogram map even in the case when the noise level is three times higher than the loop brightness.

Figures 6 and 7 show periodmaps of the data cubes of the oscillatory event on 14 July 1998, discussed in Section 2.2, in 171 and 195 Å bandpasses, respectively. The analysed signals are the running differences of the original data cube smoothed by two points in both spatial dimensions. As the periods of the detected oscillations are rather high, in the blue part of the spectrum, we process the maps with the use of the *hist_equal* function of IDL. This function returns a histogram-equalised byte array, which is then visualised with the use of *tvscl*. The transverse oscillations are clearly seen on both periodmaps as the extended regions of the same or similar colour in the parts of the map, which correspond to the boxes in the active region image shown in Figure 1. The oscillations are also well seen on the periodmaps constructed for the running differences of the original signal, without smoothing in spatial dimensions. Also, periodmaps of the original signal itself do show the oscillating regions, but they are less pronounced in this case.

Periodmaps of the data cubes of the oscillatory event on 2 July 1998, discussed in Section 2.3, in 171 and 195 Å bandpasses, are shown in Figures 8 and 9, respectively. Both periodmaps show clear evidence of the periodic motions in the regions highlighted in boxes in Figure 2. Also, in the central parts of the periodmaps, there are interesting diffuse regions with evident periodicity. Perhaps this periodicity, of about 3 min, is associated with the moss oscillations discussed in De Pontieu, Erdélyi, and de Wijn (2003).

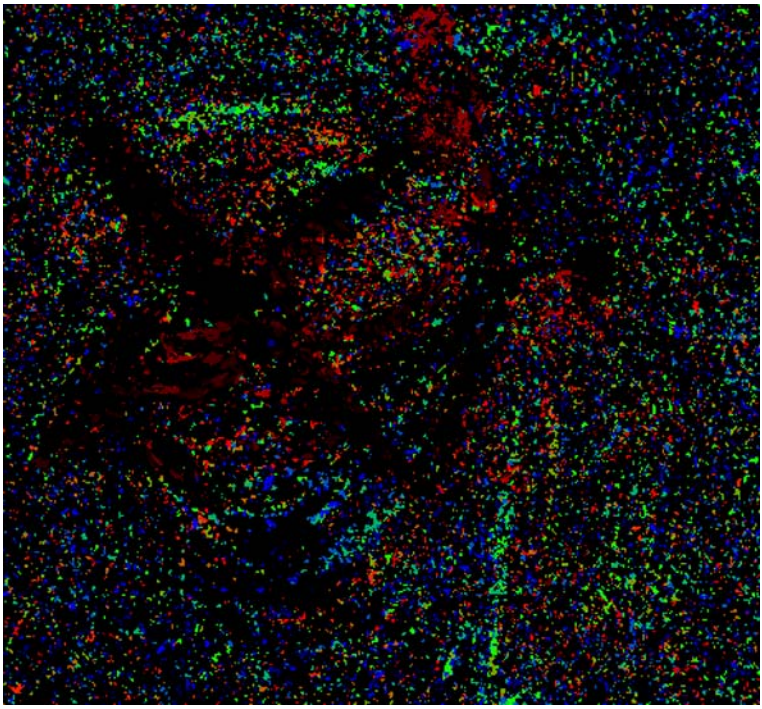

Figure 7 Periodmap of the data cube recorded by TRACE in the 195 Å bandpass for the event on 14 July 1998.

The applied colour table is not quantitatively associated with the values of the detected frequencies, as it depends upon the signal cadence time. However, for data pre-analysis purposes, the specific values of the detected frequencies are not so important, and we believe that the constructed periodmaps do not have to have a well-defined relation between colour and detected frequency.

All constructed periodmaps contain very significant noise. The noise may be reduced by either limiting the analysed frequency band (*e.g.* not considering spectral peaks, which correspond to the frequencies too close to the FFT frequency range boundaries) or increasing the prescribed detection threshold. However, these limitations may affect the detection efficiency, and we are reluctant to impose them. In any case, further studies of the optimal detection regimes for specific instruments are required.

Processing of a typical TRACE data cube consisting of 60 frames of 512^2 pixels each with a periodmap code written in the IDL takes about 40 s of computational time on an average PC (Intel Pentium M, 1.2 GHz, 504 MB of RAM). SDO/AIA full-resolution data cubes will be 4096×4096 pixels, 64 times larger than the tested data cube. Efficient application of the periodmap technique will require acceleration of the computation speed by a factor of 10. This target is achievable with the use of faster computers, conversion of the code from the interpreted language IDL to a compiled one and the implementation of multithreaded programming. The required calculation speed certainly rules out alternative pre-analysis techniques, such as the use of wavelets.

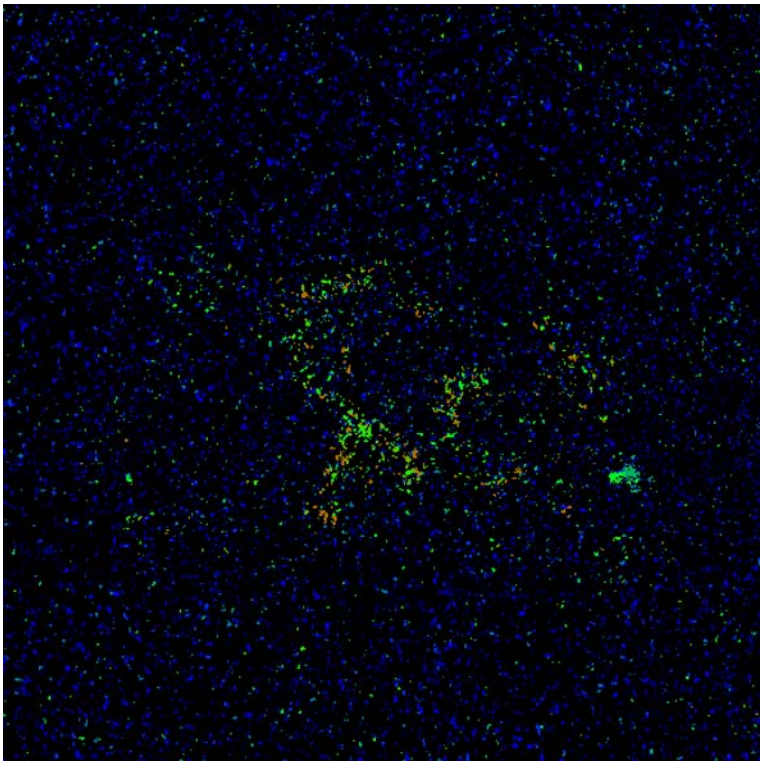

Figure 8 Periodmap of the data cube recorded by TRACE in the 171 Å bandpass for the event on 2 July 1998.

5. Discussion and Conclusions

We propose periodogram mapping of coronal EUV data cubes as a method for the pre-analysis of solar coronal EUV observations, which allows us to assess whether a certain time interval or a certain region of the corona is of interest from the point of view of searching for wave and oscillatory processes, discovered with SOHO/EIT and TRACE instruments. The method reduces a three-dimensional data cube to a two-dimensional periodmap of the cube. Each pixel on the periodmap corresponds to a spatial pixel of the analysed data cube. The colour of the pixel is assigned to be black, or another "blank" colour predetermined by the applied colour scheme, if the maximum of the power spectrum of the pixel's time signal is below a predetermined periodicity detection threshold. Otherwise, the pixel's colour corresponds to the frequency of the power spectrum maximum. Thus, information about the amplitude of the spectral maximum, if it exceeds the periodicity detection threshold, is missing. If there is a sufficiently large group of neighbouring pixels of the same or of a similar colour on the periodmap, it indicates that this particular region of the corona is of interest and requires closer inspection. In the method, the probability of a false-alarm detection is not rigorously estimated. However, it is sufficiently small because only groups of neighbouring pixels of the same or similar colour (*i.e.* groups of neighbouring pixels that have spectral maxima at the same or similar frequency) are considered to indicate the presence of a signal.

Also, we tested an alternative technique, the variance mapping technique proposed by Grechnev (2003) for the pre-analysis of microwave imaging data, in application to the search

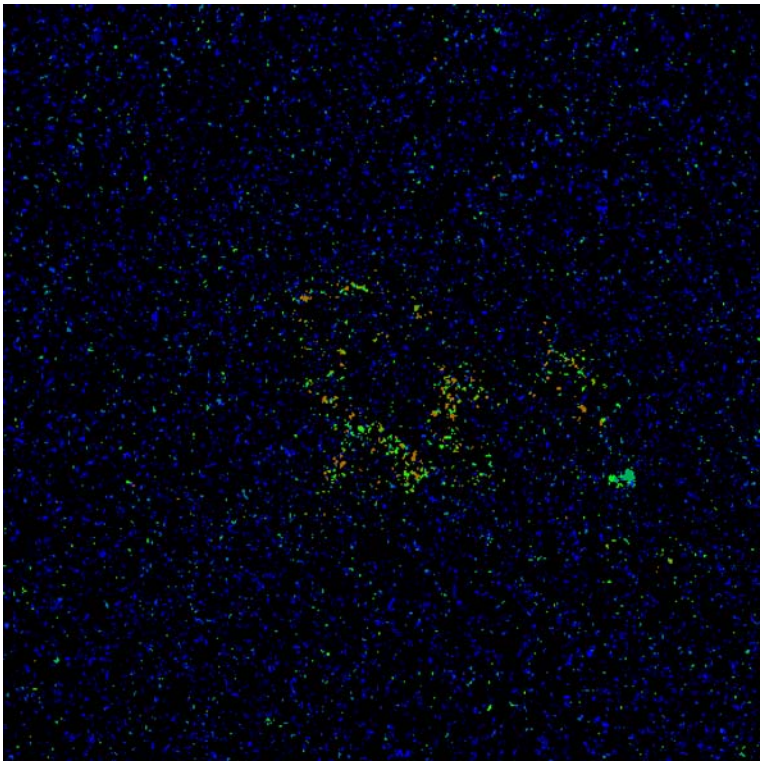

Figure 9 Periodmap of the data cube recorded by TRACE in the 195 Å bandpass for the event on 2 July 1998.

for wave and oscillatory processes in TRACE data sets. We conclude that this technique, at least in the tested form, does not give us satisfactory results for EUV data cubes because of their high variance.

We applied the periodmap technique to data cubes of two events observed by TRACE, one with clear transverse oscillations and the other with longitudinal propagating waves. Both phenomena are widespread, are considered as promising tools for coronal seismology, and are usually clearly harmonic. In both cases, the periodmaps give clear indication of the regions with the phenomena of interest.

We believe that the proposed method is sufficiently robust in its application to the predetection of EUV coronal waves and oscillations. As periodic variations of the EUV intensity connected with MHD waves and oscillations are usually quite localised in time, we do not think that an episodic missing frame or phase shifts in sampling time can noticeably affect periodicity detection. However, the robustness of the method requires further investigation.

In reality, coronal oscillation signals are modulated in both amplitude, *e.g.* damping, and in frequency, because of slow variation of physical conditions in the oscillating structures. These effects complicate the detection of an oscillation with periodmaps. It is clear that periodicity detection efficiency is affected, in particular, by the ratio of the oscillation duration to the duration of the analysed data. This suggests that long data sets should be divided into several subsets. The subset duration should be several times longer than the expected period of the oscillation. As the typical periods of coronal oscillations detected with TRACE are

several minutes, it does not seem to be practical to make the subsets shorter than 30 min. For example, for the analysis of longer data sets, lasting several hours (*e.g.* sets obtained with TRACE and expected with Hinode/XRT), or for the routine scanning of continuous full-sun data sets (*e.g.* those planned with SDO/AIA), we would suggest splitting the analysed data sets into hourly data sets that have 20 min of overlap with each other. This approach would give us a sequence of hourly periodmaps, highlighting the regions and time intervals of interest for further analysis. In general, it has been already pointed out that it is not necessary for coronal MHD waves to be clearly harmonic (see *e.g.* the discussion in Nakariakov *et al.*, 2004). However, it is not clear how the departure from harmonicity can be built into an efficient and robust automated detection technique.

The proposed technique can be considered as a more time-economical version of the wavelet spectral technique developed by De Moortel and McAteer (2004). Hence, the periodmap technique is, as is demonstrated here, suitable for the implementation in the SDO/AIA data pre-analysis and, in particular, for integration into e-SDO technology.

Acknowledgements The authors are grateful to Len Culhane, Ineke De Moortel, Erwin Verwichte, Claire Foullon, Eoghan O'Shea, Tony Arber and Victor Grechnev for stimulating discussions. The authors thank the TRACE consortia for their data.

References

Aschwanden, M.J., Fletcher, L., Schrijver, C.J., Alexander, D.: 1999, *Astrophys. J.* **520**, 880.
Aschwanden, M.J., Nightingale, R.W., Tarbell, T.D., Wolfson, C.J.: 2000, *Astrophys. J.* **535**, 1027.
De Moortel, I., McAteer, R.T.J.: 2004, *Solar Phys.* **223**, 1.
De Pontieu, B., Erdélyi, R., de Wijn, A.G.: 2003, *Astrophys. J.* **595**, L63.
Grechnev, V.V.: 2003, *Solar Phys.* **213**, 103.
Ireland, J., Walsh, R.W., Harrison, R.A., Priest, E.R.: 1999, *Astron. Astrophys.* **347**, 355.
King, D.B., Nakariakov, V.M., Deluca, E.E., Golub, L., McClements, K.G.: 2003, *Astron. Astrophys.* **404**, L1.
McAteer, R.J.T., Gallagher, P.T., Williams, D.R., Mathioudakis, M., Keenan, F.P.: 2003, *Astrophys. J.* **587**, 806.
Nakariakov, V.M., Arber, T.D., Ault, C.E., Katsiyannis, A.C., Williams, D.R., Keenan, F.P.: 2004, *Mon. Not. Roy. Astron. Soc.* **349**, 705.
Nakariakov, V.M., Ofman, L., DeLuca, E.E., Roberts, B., Davila, J.M.: 1999, *Science* **285**, 862.
Nakariakov, V.M., Verwichte, E.: 2005, *Living Rev. Solar Phys.* **2**, 3. http://www.livingreviews.org/lrsp-2005-3 (accessed 05/07/2005).
O'Shea, E.O., Banerjee, D., Doyle, J.G., Fleck, B., Murtagh, F.: 2001, *Astron. Astrophys.* **368**, 1095.
Podladchikova, O., Berghmans, D.: 2005, *Solar Phys.* **228**, 265.
Terradas, J., Molowny-Horas, R., Wiehr, E., Balthasar, H., Oliver, R., Ballester, J.L.: 2002, *Astron. Astrophys.* **393**, 637.
Title, A.M., AIA Team: 2006, *AAS/Solar Physics Division Meeting* **37**, #36.05.